2020 IEEE/RSJ International Conference on Intelligent Robots and Systems (IROS)
October 25-29, 2020, Las Vegas, NV, USA (Virtual)

Human Gait Phase Recognition using a Hidden Markov Model Framework*

Ferhat Attal[1], Yacine Amirat[1], Abdelghani Chibani[1] and Samer Mohammed[1]

Abstract— **Analysis of human daily living activities, particularly walking activity, is essential for health-care applications such as fall prevention, physical rehabilitation exercises, and gait monitoring. Studying the evolution of the gait cycle using wearable sensors is beneficial for the detection of any abnormal walking pattern. This paper proposes a novel discrete/continuous unsupervised Hidden Markov Model method that is able to recognize six gait phases of a typical human walking cycle through the use of two wearable Inertial Measurement Units (IMUs) mounted at both feet of the subject. The results obtained with the proposed approach were compared to those of well-known supervised and unsupervised segmentation approaches. The obtained results show the efficiency of the proposed approach in accurately recognizing the different gait phases of a human gait cycle. The proposed model allows the consideration of the sequential aspect of the walking gait phases while operating in an unsupervised context that avoids the process of data labeling, which is often tedious and time-consuming, particularly within a massive-data context.**

I. INTRODUCTION

Walking is a natural human locomotion mode that requires a coordinated synergy between the nervous system and the skeletal muscles involved in lower-limb movement generation [1]. Walking activity involves alternatively and repeatedly the two legs in moving the human body forward while maintaining balance during dynamic and static postures. The basic component of the walking activity is the gait cycle, which starts at the moment of initial contact of one foot with the ground and lasts until the same foot contacts the ground again. Analysis of the evolution of the gait cycle is at the core of many application fields, and is used for providing useful information for clinicians during the process of gait-rehabilitation treatment [2]; improving athlete coaching performances and preventing subject injuries [3]; and providing valuable inputs for the design and control of wearable devices such as orthoses/prostheses and exoskeletons during assistance or rehabilitation processes [4]. Gait analysis can also assist doctors in the diagnosis of certain diseases such as Parkinson's disease, and in the assessment of the risk of developing dementia [5], etc.

The use of classical tools for data gathering and treatment for gait analysis is often a tedious and time-consuming task, particularly within the context of a large amount of data. Therefore, there is a growing need for the development of automatic systems for gait analysis. Several approaches have been used in the literature to address the problem of gait analysis through the recognition/segmentation of gait phases. These approaches are related to different factors such as the nature, number and placement of sensors.

With regard to the nature of the sensors, several systems have been used in the literature, namely wearable and non-wearable systems [1]. As examples of non-wearable sensors, one can cite the video-based systems [6], [7], the floor-based systems such as pressure-measurement and force-platform systems [8] and Laser Range Finders (LRF) mounted on robotic rollators [9] or fixed at predefined locations [10]. However, these systems present some disadvantages, which are related mainly to their relatively high costs as well as the difficulties of their use in cluttered and outdoor environments. For the wearable systems, inertial measurement units and plantar pressure sensors are most commonly used [11], [12], [13]. They present several advantages over the non-wearable systems: they can be used in both indoor and outdoor environments, are less costly, and have limited sizes and energy consumption due to the latest advances in Micro-Electro Mechanical Systems (MEMS).

Different methods have been used in the literature to address the problem of automatic gait recognition. In [14], a threshold-based method and a smart shoe equipped with inertial and force sensors are used to recognize four gait phases. In [15], a threshold-based method is also used to recognize four gait phases, using data provided by three foot switches placed under the sole of the foot. In [16], data collected from a 3D magnetometer placed at the subject's shank and a threshold-based method are used to recognize four gait phases. The main limitation of threshold-based methods is related to the choice of thresholds that are chosen empirically based on observational analysis, which may affect their generalization. With regard to machine-learning-based methods for gait-phase assessment, several approaches have been used in the literature. In [17], a fuzzy inference system is used to detect abnormalities in the gait-phase transition, as well as for the recognition of six gait phases using GRF data collected from four air-pressure sensors embedded in the subject's shoes. In [18], a Hidden Markov Model (HMM) is used to recognize the six gait phases using the GRF data provided by smart shoes equipped with four air-pressure sensors. A HMM is also used in [19] to recognize four gait phases using data collected from gyroscope sensors mounted at the foot level. In [11], a supervised HMM is used to classify six gait phases using GRF data provided by in-shoe pressure sensors. In [9], a

*This work was not supported by any organization

[1] F. Attal, Y. Amirat, A. Chibani and S. Mohammed are with University Paris-Est Créteil (UPEC), LISSI, 122 rue Paul Armangot, 94400, Vitry-Sur-Seine, France ferhat.attal@u-pec.fr, amirat@u-pec.fr, abdelghani.chibani@u-pec.fr, samer.mohammed@u-pec.fr.

supervised HMM is used to recognize seven gait phases through data measured by a Laser Range Finder sensor mounted on a robot walker that follows the subject. In [13], a supervised HMM is used to classify four gait phases using data collected from a gyroscope mounted on each foot of the subject. A supervised HMM is also proposed in [20] to recognize i) two gait phases, ii) four gait phases, and iii) six gait phases using data provided by gyroscope sensors placed at the foot and shank of the subject's leg. In [21], a hybrid neural network and HMM, in supervised framework, are combined to recognize six gait phases using data collected from inertial sensing and optical motion capture systems. In [22], curve similarity model and ground contact forces data are used to distinguish between swing phase and stance phase in real time context. Most of the aforementioned studies used supervised classification techniques, which require labeled data and do not consider the temporal aspect of the data. In [23], switching linear dynamical systems and joint angle kinematic data are used to model four gait phases. In our previous works [24], a Multiple Regression Hidden Markov Model (MRHMM) was proposed to segment gait cycle into six gait phases using vGRF signals collected from in-shoe pressure sensors. These sensors present several advantages such as accuracy measurement and low cost; they have, however, some disadvantages such as: a bad linearity, a complex signal processing, and limited life expectancy. In addition, from model point of view, in [24], the use of regressive version of HMM is related to the fact that the vGRF signals follow a polynomial evolution according to gait phases, which can be easily modeled using polynomial functions through a regressive model.

In this study, we propose a discrete/continuous unsupervised HMM approach, which combines a HMM-based model with the use of acceleration data acquired during multiple gait cycles. The parameters of the generated model are learned in an unsupervised way from unlabeled raw acceleration data acquired during the human gait using the Baum-Welch algorithm [25]. The most likely sequence of gait phases is then estimated using the Viterbi algorithm [26]. Six gait phases are considered in this study: loading response, mid-stance, terminal stance, pre-swing, mid-swing and terminal swing. Four performance criteria were used to assess the proposed approach: accuracy, F-measure, recall and precision.

The rest of the paper is organized as follows: Section II presents a description of the human gait cycle and its subsequent phases, as well as the experimental protocol and data-labeling process. Section III presents the proposed gait-cycle phase-recognition approach. The performance of the proposed approach is compared to those of traditional supervised and unsupervised machine-learning approaches and discussed in section IV. Section V concludes the paper and presents some potential research perspectives.

II. Data Collection

A. Human gait cycle

The human gait cycle is a cyclic pattern, that is characterized by two main phases: the stance phase and the swing phase. The stance phase represents approximately 60% of the whole gait cycle, while the swing phase represents approximately 40%. Generally, the gait cycle starts from the heel strike of one foot with the ground and ends when the heel of the same foot contacts the ground again. According to [27], the walking gait cycle involves eight phases: initial contact (IC), loading response (LR), mid-stance (MS), terminal stance (TS), pre-swing (PSW), initial swing (ISW), mid-swing (MSW) and terminal swing (TSW). In this study, a configuration that includes six gait phases (LR, MS, TS, PSW, ISW, MSW and TSW) is considered. Fig.1 illustrates the considered gait phases.

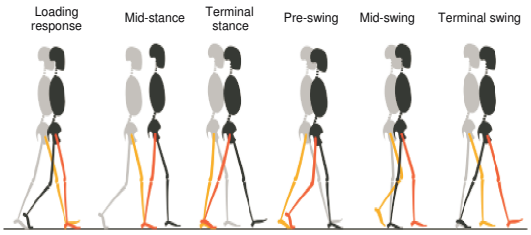

Fig. 1. Gait-phase illustration

B. Experimental protocol for data acquisition and data labeling

1) Data acquisition: In this study, the gait-cycle phases are classified using two MTx 3-DOF inertial measurement units (IMUs) from Xsens mounted at each foot of the subject, as shown in Fig. 2. Each MTx unit is equipped with a tri-axial accelerometer/gyrometer, which measures the acceleration and angular velocity in 3D space. The MTx inertial trackers are connected via an Xbus cable to the central unit, called the Xbus Master, which is attached to the waist of the subject. The collected data are transmitted to the host computer through a wireless Bluetooth link. The sampling frequency is set to 100 Hz, which is large enough to assess the human gait cycle. The experiments were performed at the LISSI

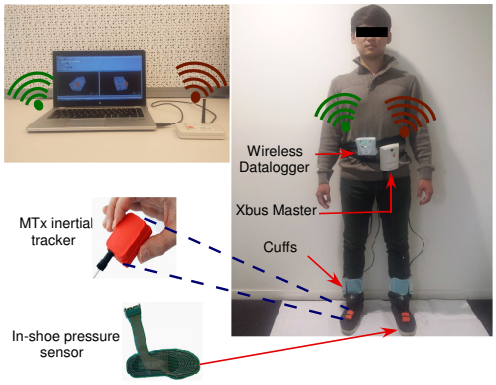

Fig. 2. Placement of inertial and pressure sensors.

Lab of the University of Paris-Est Creteil (UPEC) with five healthy subjects with different profiles (mean age: 27 years old, mean weight: 79 kg). Each subject was asked to perform

thirty cycles along a straight line on his own style. Fig. 3 shows the evolution of the acceleration data of both the left and right feet during five walking cycles.

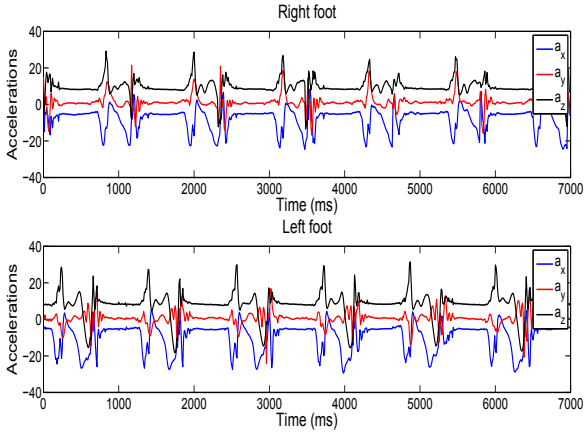

Fig. 3. Example of 3D acceleration data, collected during five walking cycles.

2) Data labeling: To evaluate the performance of the proposed approach, a data-labeling step was carried out during the experimental process. To accurately estimate the different time intervals of each gait phase, a pressure-based mapping system from Tekscan, also known as the F-Scan Wireless in-shoe pressure-mapping system, is used. This system consists of in-shoe pressure sensors, a Wireless Datalogger unit and Cuffs, as shown in Fig. 2. The Wireless Datalogger unit acts as a wireless gateway between the Cuffs, the in-shoe pressure sensors and the host computer; see Fig. 2. The data labeling is performed manually by analyzing the vertical Ground Reaction Force (vGRF) profiles collected from the in-shoe pressure sensors [11].

III. HMM-BASED GAIT-CYCLE PHASE-RECOGNITION METHODOLOGY

A. Hidden Markov Model background

Hidden Markov Model (HMM) is a powerful tool for analyzing time-series data and has been used in many applications. The HMM is a doubly stochastic process [28] and assumes that the underlying Markov process is not directly observable (hidden states) but could be observable through other stochastic processes. This model consists of a structure that is composed of states, transition probabilities, and a set of probability distributions, which can be discrete or continuous, depending on the observation type. In the case of a Discrete HMM (DHMM), observations are discrete symbols from a finite alphabet. A DHMM is defined by a quintuplet $\lambda = (N, M, A, B, \pi)$, where:

- N represents the number of hidden states in the model. Let us denote by $S = \{s_1, s_2, s_3, \ldots, s_N\}$ the state vector, where the state s_i at time t is defined by the variable q_t.
- M denotes the number of distinct observations per state. Let us denote by $V = \{v_1, v_2, v_3, \ldots, v_M\}$ the observation vector.
- The transition probability distribution matrix is denoted by $A = \{a_{ij}\}$, where

$$a_{ij} = P(s_j = q_{t+1} | s_i = q_t), 1 \leq i, j \leq N. \quad (1)$$

- The observation probability distribution matrix in state j is denoted by $B\{b_j(k)\}$, where

$$b_j(k) = P(v_k | s_j = q_t), 1 \leq j \leq N, 1 \leq k \leq M. \quad (2)$$

- The initial probability distribution is denoted by $\pi = \{\pi_i\}$, where:

$$\pi_i = P(s_i = q_1), 1 \leq i \leq N \quad (3)$$

Compact notation is often used in the literature to define the complete parameter set of the model, such as $\lambda = \{A, B, \pi\}$.

In the case of a Continuous HMM (CHMM), observations have continuous values. Therefore, to ensure that the model parameters are re-estimated in a consistent way, some restrictions on the form of the probability density function (pdf) have to be considered. In the literature, the most commonly used form of pdf is the finite mixture see equation (4).

B. Gait-cycle phase recognition using a Hidden Markov Model

The different steps of the gait-cycle phase-recognition process are shown in Fig. 4. To recognize the six gait phases

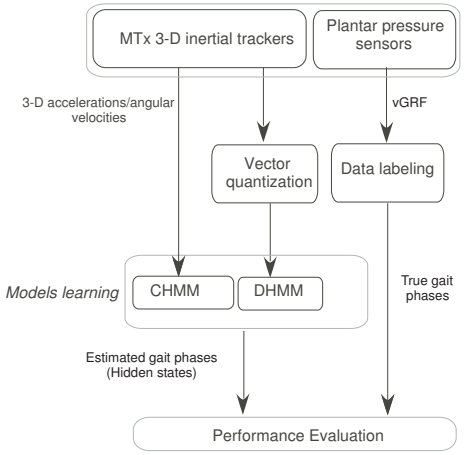

Fig. 4. Gait-cycle phase-recognition methodology.

considered in section II, a discrete/continuous unsupervised HMM is used with a six-state left-to-right topology; each state corresponds to a gait phase. This topology is well suited to the model of normal walking gait due to the sequential evolution of the gait phases [9]. In the following, DHMM and CHMM refer, respectively, to the use of HMM within discrete-observation and continuous-observation contexts.

CHMM: The emission distributions for each state are modeled using a multivariate Gaussian distribution, such as

$$b_j(X) = \sum_{m=1}^{M} c_{jm} \mathcal{N}\left[X, \mu_{jm}, \Sigma_{jm}\right], \quad (4)$$

where: c_{jm} represents the mixture coefficient for the m^{th} mixture in state j; $\mathcal{N}$ represents the multivariate Gaussian density; μ_{jm} represents the mean vector for the m^{th} mixture in state j; Σ_{jm} represents the covariance matrix for the m^{th} mixture in state j.

As the number of states is equal to 6, the only parameter to tune is the number of mixtures M. This number reflects a trade-off between the complexity of the model structure and the performance of the model in terms of recognition rate. In this study, each state is modeled using a mixture of 3 diagonal Gaussians.

DHMM: To use the DHMM, the continuous observations are transformed into discrete observations using the Vector Quantization (VQ) method. It allows a continuous-amplitude signal to be approximated by a discrete-amplitude signal. Formally, it can represent any vector $X \subseteq \mathbb{R}^d$ by another vector $V = \{v_1, v_2, v_3, \ldots, v_M\}$ using a code book $C = \{C_1, C_2, C_3, \ldots, C_M\}$ in $\mathbb{R}^d$ of M vectors, where $C_i = \{c_1, c_2, \ldots c_d\}$ is the i^{th} code word; and $\mathbb{R}^d$ is d-dimensional Euclidean space. K-means is one of the most simple and efficient algorithms for constructing a code book from unknown data. This algorithm has as input the matrix of accelerations and angular velocities, and as output the vector of discrete observations V. The code-book size of 40 elements provides the best trade-off between error quantification and performance of the model in terms of recognition rate.

The DHMM and CHMM parameters are estimated using the Baum-Welch algorithm [28]. Regarding the inference problem, the Viterbi decoding algorithm is used to estimate the state sequence, i.e., the gait phases.

IV. Experimental results

A. Results and discussions

To evaluate the performance of the proposed gait phase-recognition approach, four criteria are used: accuracy, F-measure, recall and precision. Table I summarizes the recognition rates obtained with each subject using CHMM and DHMM. The obtained results show the ability of the HMM to recognize accurately the different walking gait phases. We note that, in the case of CHMM, the recognition rates are higher than 79.30%, with an average accuracy of 82.62%. In the case of DHMM, the recognition rates are higher than 79.30%, with an average accuracy of 78.25%. The obtained results in terms of F_1-measure per class, F_1-measure, precision, recall, average accuracy and its standard deviation are shown in Table II. It should be noted that CHMM gives better results than DHMM, which can be explained by the fact that, in the case of DHMM, a transformation of the continuous observations into discrete observations is needed. This transformation may lead to information loss, which can affect the prediction quality of the model. The global confusion matrices obtained with CHMM and DHMM are given in Tables III and IV, respectively. The LR phase is estimated with an accuracy of 95.83% in the case of CHMM, while in the case of DHMM, the same phase is recognized with an accuracy of 93.13%. In the case of CHMM, confusions occur between: (i) MS and TS phases with a confusion rate of 20.58%, (ii) TS and PSW phases with a confusion rate of 14.43%, and (iii) MSW and TSW phases with a confusion rate of 15.95%. In the case of DHMM, confusions occur chiefly between: (i) MS and TS phases with a confusion rate of 16.11%, (ii) TS and PSW with a confusion rate of 13.30%, (iii) PSW and MSW with a confusion rate of 13.87%, and (iv) MSW and TSW phases with a confusion rate of 23.48%. These confusions can be explained by the fact that the reference (true) labels are constructed manually. The reference labels may not be accurate enough to be considered real labels, especially during transitions between phases. Fig. 5 represents the estimated phases obtained with CHMM and DHMM for five gaits, along with the reference hand-labeled data. We notice that the hidden states, i.e., the recognized phases, for both CHMM and DHMM follow a sequential evolution that is in accordance with the walking gait phases. Moreover, DHMM and CHMM provide accurate data segmentation with respect to the reference labels. In some cases, the recognized phases do not match the reference labels. This phenomenon usually occurs during transitions between phases since the walking gait phases are modeled using a HMM with left-to-right topology.

TABLE I
Recognition rates for each subject

	CHMM	DHMM
$Subject_1$ (%)	85.31	80.80
$Subject_2$ (%)	84.91	78.35
$Subject_3$ (%)	82.18	77.28
$Subject_4$ (%)	79.30	77.02
$Subject_5$ (%)	80.66	76.85

B. Comparison with unsupervised and supervised classification approaches

In this section, the performance of the proposed approach is compared to those of standard supervised and unsupervised machine-learning approaches. In supervised approaches, the labels are used in the learning phase to construct the models. The leave-one-out evaluation method is used to construct the learning dataset and the testing dataset. The latter is composed of data collected from one subject, while the former is composed of data collected from the remaining subjects. This procedure is repeated for each subject. In unsupervised approaches, no labels are used to construct the models, which are learned without using any labels. The labels are used only to evaluate the performances of the considered approaches. The model parameters of each approach are chosen in such way that maximizes their recognition performance rates.

F_1-measure per class, F_1-measure, precision, recall, average accuracy and its standard deviation, obtained with re-

TABLE II

F_1-MEASURE PER CLASS, F_1-MEASURE, PRECISION, RECALL, AND AVERAGE OF ACCURACY RATE (R) AND ITS STANDARD DEVIATION (STD) FOR EACH MODEL

	F_1 measure per class						F_1 measure	Precision	Recall	Accuracy
	1	2	3	4	5	6				$(R) \pm (std)$
DHMM (%)	92.45	79.30	74.88	76.07	67.83	79.01	78.28	78.25	87.32	78.25 ± 1.63
CHMM (%)	92.58	80.87	79.18	79.58	76.55	86.73	82.71	82.62	82.79	82.62 ± 2.61

TABLE III

GLOBAL CONFUSION MATRIX OBTAINED WITH CHMM

		Obtained classes					
		LR	MS	TS	PSW	MSW	TSW
True classes	LR (%)	95.83	4.16	0	0	0	0
	MS (%)	11.19	84.68	4.12	0	0	0
	TS (%)	0	20.58	77.70	1.70	0	0
	PSW (%)	0	0	14.43	75.00	10.56	0
	MSW (%)	0	0	0	11.77	78.45	9.76
	TSW (%)	0	0	0	0	15.95	84.05

TABLE IV

GLOBAL CONFUSION MATRIX OBTAINED WITH DHMM

		Obtained classes					
		LR	MS	TS	PSW	MSW	TSW
True classes	LR (%)	93.13	6.86	0	0	0	0
	MS (%)	8.34	80.80	10.85	0	0	0
	TS (%)	0	16.11	74.31	9.57	0	0
	PSW (%)	0	0	13.30	75.77	10.92	0
	MSW (%)	0	0	0	13.87	68.98	17.13
	TSW (%)	0	0	0	0	23.48	76.51

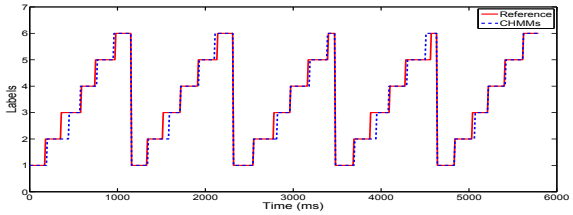

(a)

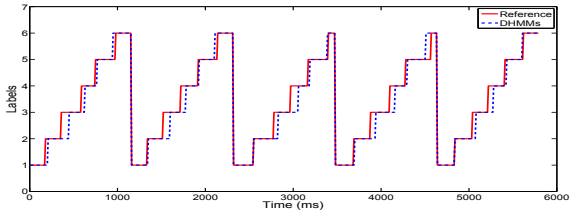

(b)

Fig. 5. Gait-phase evolutions obtained with (a) CHMM and (b) DHMM

spect to standard unsupervised and supervised classification approaches, are summarized in Table V. The proposed HMM approach outperforms the standard ones, as it achieves accuracy rates of 78.25% and 82.62% with DHMM and CHMM, respectively, while only 42.96% and 59.43% of instances are well classified using K-Means and GMM, respectively. Note that the unsupervised GMM and K-means approaches are not well suited for this kind of sequential data as they do not consider the sequential and temporal aspects in their model formulations. It can also be observed that Random Forest (RF) achieves the highest classification accuracy rate of 88.33%, followed by the k-Nearest Neighbors (k-NN), with an accuracy rate of 84.73%. Support Vector Machine (SVM) and Multi-Layer Perceptron (MLP) obtain accuracy rates of 83.89% and 80.50%, respectively. The supervised learning model SLGMM obtains an accuracy rate of 79.49%, and Naive Bayes (NB) obtains the lowest accuracy rate of 75.68%. Table V shows also that the RF approach achieves the best performance in terms of F_1-measure per class, F_1-measure, precision, recall, and average accuracy. Compared to standard supervised classification techniques, the proposed HMM techniques outperform some of them with an accuracy rate of 82.62% in the case of CHMM, while only 79.49% and 75.68% of instances are well classified using the supervised GMM and the NB approaches, respectively. One can notice also that the results obtained with CHMM are almost the same as those obtained with the K-NN and MLP approaches. The obtained results are very encouraging since the proposed approach performs within an unsupervised context. Furthermore, the aforementioned supervised classification approaches require a labeled collection of data for training. In addition, they do not explicitly include the temporal dependence in their model formulations. Globally, unlike supervised-based classifiers, which require labeled data in the model-training phase, the proposed approach shows very encouraging results since it does not require any labeled data, while it considers temporal and sequential aspects of the acquired data.

V. CONCLUSION AND PERSPECTIVES

In this paper, we presented a human walking gait phase-recognition approach based on the use of only two inertial measurement units, which are worn by a subject at the foot level. A discrete/continuous unsupervised HMM with a left-to-right topology is used to model the sequential appearance of the walking gait-cycle phases as well as the transitions between those phases. The use of HMM in an unsupervised context is very useful for classifying a large amount of unlabeled data into different gait-cycle phases. The obtained results with healthy subjects are satisfactory and clearly show the efficiency of the proposed approach by comparison to well-known supervised and unsupervised machine-learning-based approaches. This work can be extended in several directions. Feature extraction/selection from raw inertial data

TABLE V

COMPARISON OF THE PERFORMANCE IN TERMS OF ACCURACY, RECALL, PRECISION AND F_1 MEASURE OF THE FIVE SUPERVISED CLASSIFIERS AND TWO UNSUPERVISED CLASSIFIERS

	F_1 measure per class						F_1 measure	Precision	Recall	Accuracy
	1	2	3	4	5	6				$(R) \pm (std)$
k-NN (%)	86.76	85.51	84.58	80.66	83.13	87.68	84.76	84.73	84.78	84.73 ± 2.13
SVM (%)	87.29	84.28	83.61	81.07	81.89	85.14	83.91	83.89	83.93	83.89 ± 1.91
Naive Bayes (%)	82.50	77.86	68.21	72.84	72.53	79.72	75.97	75.68	76.25	75.68 ± 1.78
Random Forest (%)	90.49	87.93	87.42	87.76	87.08	89.26	88.34	88.33	88.36	88.33 ± 1.72
MLP (%)	73.80	84.23	80.03	81.71	84.33	81.41	81.91	80.50	83.36	80.50 ± 2.35
SLGMM (%)	85.42	81.68	77.43	76.47	74.99	80.75	79.74	79.49	79.99	79.49 ± 2.48
k-Means (%)	35.60	41.21	53.88	28.68	39.22	61.06	45.28	42.96	47.86	42.96 ± 7.56
GMM (%)	54.22	57.63	59.69	42.23	66.32	73.90	59.38	59.43	59.33	59.43 ± 7.02

can be introduced in the recognition process to improve the classification accuracy rate. To evaluate the robustness of the proposed methodology and its effectiveness for the diagnosis of neurodegenerative diseases such as Parkinson's disease, the ongoing works concern the enrichment of database by data from healthy subjects as well as subjects with diseases affecting walking; walking data collected in the context of various gait speeds will also be considered.

REFERENCES

[1] J. Taborri, E. Palermo, S. Rossi, and P. Cappa, "Gait partitioning methods: A systematic review," *Sensors*, vol. 16, 2016.

[2] J. F. Veneman, R. Kruidhof, E. E. Hekman, R. Ekkelenkamp, E. H. Van Asseldonk, and H. Van Der Kooij, "Design and evaluation of the lopes exoskeleton robot for interactive gait rehabilitation," *IEEE Transactions on Neural Systems and Rehabilitation Engineering*, vol. 15, no. 3, pp. 379–386, 2007.

[3] A. Santuz, A. Ekizos, and A. Arampatzis, "A pressure plate-based method for the automatic assessment of foot strike patterns during running," *Annals of biomedical engineering*, vol. 44, no. 5, pp. 1646–1655, 2016.

[4] W. Hassani, S. Mohammed, and Y. Amirat, "Real-time emg driven lower limb actuated orthosis for assistance as needed movement strategy." in *Procedings of the Robotics: Science and Systems Conference*, 2013.

[5] X. Meng, H. Yu, and M. P. Tham, "Gait phase detection in able-bodied subjects and dementia patients," in *Proceedings of the IEEE International Conference on Engineering in Medicine and Biology Society*, 2013, pp. 4907–4910.

[6] A. Kale, A. Rajagopalan, N. Cuntoor, and V. Kruger, "Gait-based recognition of humans using continuous hmms," in *Proceedings of the 5th IEEE International Conference on Automatic Face and Gesture Recognition*, 2002, pp. 336–341.

[7] A. Miller, "Gait event detection using a multilayer neural network," *Gait & posture*, vol. 29, no. 4, pp. 542–545, 2009.

[8] L. Ballaz, M. Raison, C. Detrembleur *et al.*, "Decomposition of the vertical ground reaction forces during gait on a single force plate," *Journal of musculoskeletal and neuronal interactions*, vol. 13, no. 2, pp. 236–243, 2013.

[9] X. S. Papageorgiou, G. Chalvatzaki, C. S. Tzafestas, and P. Maragos, "Hidden markov modeling of human normal gait using laser range finder for a mobility assistance robot," in *Proceedings of the IEEE International Conference on Robotics and Automation*, 2014, pp. 482–487.

[10] T. Pallejà, M. Teixidó, M. Tresanchez, and J. Palacín, "Measuring gait using a ground laser range sensor," *Sensors*, vol. 9, no. 11, pp. 9133–9146, 2009.

[11] S. De Rossi, S. Crea, M. Donati, P. Reberšek, D. Novak, N. Vitiello, T. Lenzi, J. Podobnik, M. Munih, and M. Carrozza, "Gait segmentation using bipedal foot pressure patterns," in *Proceedings of the 4th IEEE RAS & EMBS International Conference on Biomedical Robotics and Biomechatronics (BioRob)*, 2012, pp. 361–366.

[12] A. Rampp, J. Barth, S. Schulein, K.-G. Gasmann, J. Klucken, and B. M. Eskofier, "Inertial sensor-based stride parameter calculation from gait sequences in geriatric patients," *IEEE Transactions on Biomedical Engineering*, vol. 62, no. 4, pp. 1089–1097, 2015.

[13] A. Mannini and A. M. Sabatini, "A hidden markov model-based technique for gait segmentation using a foot-mounted gyroscope," in *Proceedings of the IEEE Annual International Conference on Engineering in Medicine and Biology Society*, 2011, pp. 4369–4373.

[14] N. Carbonaro, F. Lorussi, and A. Tognetti, "Assessment of a smart sensing shoe for gait phase detection in level walking," *Electronics*, vol. 5, no. 4, p. 78, 2016.

[15] V. Agostini, G. Balestra, and M. Knaflitz, "Segmentation and classification of gait cycles," *IEEE Transactions on Neural Systems and Rehabilitation Engineering*, vol. 22, no. 5, pp. 946–952, 2014.

[16] S. Bonnet and P. Jallon, "Hidden markov models applied onto gait classification," in *Proceedings of the 18th European Conference on Signal Processing*, 2010, pp. 929–933.

[17] K. Kong and M. Tomizuka, "A gait monitoring system based on air pressure sensors embedded in a shoe," *IEEE Transactions on Mechatronics*, vol. 14, no. 3, pp. 358–370, 2009.

[18] J. Bae and M. Tomizuka, "Gait phase analysis based on a hidden markov model," *Mechatronics*, vol. 21, no. 6, pp. 961–970, 2011.

[19] N. Abaid, P. Cappa, E. Palermo, M. Petrarca, and M. Porfiri, "Gait detection in children with and without hemiplegia using single-axis wearable gyroscopes," *PLoS One*, vol. 8, no. 9, 2013.

[20] J. Taborri, E. Scalona, E. Palermo, S. Rossi, and P. Cappa, "Validation of inter-subject training for hidden markov models applied to gait phase detection in children with cerebral palsy," *Sensors*, vol. 15, no. 9, pp. 24 514–24 529, 2015.

[21] H. Zhao, Z. Wang, S. Qiu, J. Wang, F. Xu, Z. Wang, and Y. Shen, "Adaptive gait detection based on foot-mounted inertial sensors and multi-sensor fusion," *Information Fusion*, vol. 52, pp. 157–166, 2019.

[22] H. Hu, J. Zheng, E. Zhan, and L. Yu, "Curve similarity model for real-time gait phase detection based on ground contact forces," *Sensors*, vol. 19, no. 14, p. 3235, 2019.

[23] L. Drnach, I. Essa, and L. H. Ting, "Identifying gait phases from joint kinematics during walking with switched linear dynamical systems," in *Proceedings of the 7th IEEE International Conference on Biomedical Robotics and Biomechatronics (Biorob)*. IEEE, 2018, pp. 1181–1186.

[24] F. Attal, Y. Amirat, A. Chibani, and S. Mohammed, "Automatic recognition of gait phases using a multiple-regression hidden markov model," *IEEE/ASME Transactions on Mechatronics*, vol. 23, no. 4, pp. 1597–1607, 2018.

[25] L. E. Baum and T. Petrie, "Statistical inference for probabilistic functions of finite state markov chains," *The annals of mathematical statistics*, pp. 1554–1563, 1966.

[26] A. J. Viterbi, "Error bounds for convolutional codes and an asymptotically optimum decoding algorithm," *IEEE Transactions on Information Theory*, vol. 13, no. 2, pp. 260–269, 1967.

[27] J. Perry, J. R. Davids *et al.*, "Gait analysis: normal and pathological function." *Journal of Pediatric Orthopaedics*, vol. 12, no. 6, 1992.

[28] L. R. Rabiner, "A tutorial on hidden markov models and selected applications in speech recognition," in *Proceedings of the IEEE*, 1989, pp. 257–286.